PPP1R14D promotes the proliferation, migration and invasion of lung adenocarcinoma via the PKCα/BRAF/MEK/ERK signaling pathway

HUIJUN CAO[1*], ZHIQIANG WANG[2*], YING WANG[1], LIJUAN YE[3], RUILEI LI[1], YUANBO XUE[1], KE LI[1], TIANNAN DI[1], TAO LI[1], ZONGLIN FAN[1], YANYAN LIU[4], JIYIN GUO[1], HONG YAO[1] and CHUNLEI GE[1]

[1]Department of Cancer Biotherapy Center, Yunnan Cancer Hospital, The Third Affiliated Hospital of Kunming Medical University; [2]Department of Radiotherapy Oncology, The First Affiliated Hospital of Kunming Medical University; [3]Department of Pathology, Yunnan Cancer Hospital, The Third Affiliated Hospital of Kunming Medical University; [4]Department of Medical Oncology, Yunnan Cancer Hospital, The Third Affiliated Hospital of Kunming Medical University, Kunming, Yunnan 650000, P.R. China

Received June 6, 2022; Accepted October 6, 2022

DOI: 10.3892/ijo.2022.5443

Abstract. Protein phosphatase 1 (PP1) inhibitors play a role in tumor progression through different mechanisms. Protein phosphatase 1 regulatory subunit 14D (PPP1R14D) is an inhibitor of PP1. However, the role of PPP1R14D in tumors and its mechanism of action are largely unknown. The purpose of the present study was to investigate the expression, function and mechanism of PPP1R14D in lung adenocarcinoma (LUAD). In the present study, GEPIA database analysis and immunohistochemistry demonstrated that PPP1R14D was highly expressed in LUAD tissues and that the expression of PPP1R14D in LUAD was negatively correlated with the age of patients and positively correlated with the 8th American Joint Committee on Cancer staging among patients. In addition, Kaplan-Meier Plotter database analysis showed that PPP1R14D expression was associated with lower survival rates in patients with LUAD. PPP1R14D knockdown significantly inhibited LUAD cell proliferation, migration and invasion and induced LUAD cell arrest at the G1 phase of the cell cycle. Mechanistic analyses revealed that PPP1R14D knockdown may inhibit cell proliferation, migration and invasion by inactivating PKCα/BRAF/MEK/ERK pathway signaling and its downstream key proteins c-Myc/Cyclin E1-CDK2 and MMP2/MMP9/Vimentin. Moreover, knockdown of PPP1R14D suppressed tumor growth *in vivo*. All these results showed that PPP1R14D plays an important role in LUAD tumorigenesis and may serve as a potential prognostic factor and therapeutic target in LUAD.

Correspondence to: Dr Hong Yao or Ms. Chunlei Ge, Department of Cancer Biotherapy Center, Yunnan Cancer Hospital, The Third Affiliated Hospital of Kunming Medical University, 519 Kunzhou Road, Xishan, Kunming, Yunnan 650000, P.R. China
E-mail: yaohong20055@hotmail.com
E-mail: gechunlei1006@163.com

*Contributed equally

Key words: protein phosphatase 1 regulatory subunit 14D, lung adenocarcinoma, proliferation, migration, invasion

Introduction

Lung cancer is the second most common cancer in the world, with an incidence of 11.4%, which is only lower than that of female breast cancer. In addition, lung cancer has the highest mortality rate among all cancers, reaching 18% (1). Non-small cell carcinoma (NSCLC) accounts for 85% of all lung cancer cases, and lung adenocarcinoma (LUAD) is the most common NSCLC subtype, with an incidence of more than 40% (2). Most LUAD patients are diagnosed at an advanced stage, and the 5-year survival rate with conventional radiation and chemotherapy is only ~5% (3). In recent years, patients have benefited from immunotherapy and targeted therapy, but the 5-year survival rate for LUAD remains less than 20% (4).

For immunotherapy, an immune checkpoint inhibitor (ICI) represented by a programmed death-1 (PD-1)/programmed death ligand-1 (PD-L1) inhibitor only causes long-term remission in 20-30% of patients, followed by an easy induction of immune-related adverse events (5). All these factors restrict the clinical application of ICIs. Targeted therapies offer patients another hope. Genetic alterations play a key role in the development, progression and prognosis of LUAD, leading to uncontrolled growth and metastasis of LUAD (6). LUAD-related target genes, including EGFR, ALK, RET and ROS1, have been reported, and the treatment of these targets in LUAD has also received increasing attention with promising clinical results (4,7). However, due to the limitation of targeting and resistance to targeted drugs, the overall prognosis of patients with LUAD remains poor (4,8). Therefore, it is necessary to further explore the core regulatory targets involved in the development of LUAD and their potential mechanisms.

The extracellular signal-regulated kinase/mitogen-activated protein kinase (ERK/MAPK) signaling pathway is activated in numerous cancers, including lung cancer, and is involved

in regulating the proliferation, survival, invasion, apoptosis and drug resistance of cancer cells (9-11). In addition to being overactivated by RAS proteins, the ERK/MAPK signaling pathway is also overactivated by the α subtype of protein kinase C (PKCα) in cancer (12-14). Currently, RAF and MEK inhibitors targeting the ERK/MAPK signaling pathway only improve a small number of clinical outcomes of patients (12). However, the development of inhibitors of the upstream activating proteins of the ERK/MAPK signaling pathway has been challenging, such as the KRAS target, which has not been available for the past four decades (15). Therefore, it is necessary to identify which oncogenes are involved in the regulation of the ERK/MAPK pathway or its upstream activating proteins.

Protein phosphatase 1 regulatory subunit 14D (PPP1R14D) is normally widely expressed in the brain and intestine. The protein encoded by PPP1R14D not only determines the substrate specificity of protein phosphatase 1 (PP1), but is also activated by PKC phosphorylation to become an effective inhibitor of protein phosphatase (16,17). PP1, one of the most important Ser/Thr protein phosphatases in eukaryotic cells, is involved in numerous cellular physiological processes, including cell division and cancer development, through dephosphorylation by shedding phosphate groups on Ser/Thr residues. Recent studies have shown that PPP1R14D may play a carcinogenic role in tumors. Zhang *et al* (18) considered that proto-oncogenes can be activated through hypomethylation, and they demonstrated that PPP1R14D is hypomethylated in pancreatic cancer. Dang *et al* (19) suggested that uncontrolled cutting of cell surface and extracellular proteins by metalloproteinase will lead to tumor progression, and PPP1R14D is necessary to induce metalloproteinase ADAM17 to cut oncogenic TGF-α. However, the role of PPP1R14D in lung cancer and its underlying mechanisms are poorly understood.

In the present study, it was demonstrated that PPP1R14D is highly expressed in LUAD and that PPP1R14D may promote the proliferation, migration and invasion of LUAD by activating the PKCα/BRAF/MEK/ERK signaling pathway, thereby contributing to the poor prognosis of LUAD.

Materials and methods

GEPIA analysis. GEPIA (http://gepia.cancer-pku.cn/), an online database including LUAD (T=483; N=347) and lung squamous cell carcinoma (LUSC) (T=486; N=338) mRNA expression data from The Cancer Genome Atlas (TCGA) database and Genotype Tissue Expression (GTEx) projects, was used to analyze PPP1R14D expression between tumor and normal samples (unpaired date from different patients). This tool uses normalized mRNA levels as transcripts per million (TPM) and unpaired Student's t-test. $P<0.05$ was considered to indicate a statistically significant difference.

Survival analysis. Kaplan-Meier plotter (www.kmplot.com), an online database including gene expression data and clinical data, was used to calculate the survival time in LUAD and LUSC patients with PPP1R14D in each dataset. The survival probability, including overall survival (OS) and progression-free survival (PFS) time, was evaluated for patients with high or low mRNA expression levels of PPP1R14D, based on the best group separation. The log-rank test was used and $P<0.05$ was considered to indicate a statistically significant difference.

Tissue specimens. A total of 128 patients who underwent pulmonary adenocarcinoma resection in the Third Affiliated Hospital of Kunming Medical University from December 2008 to June 2016 were included in the study. None of the patients received preoperative radiotherapy, chemotherapy or other related antitumor therapy. LUAD tissue and matched normal lung tissue obtained during surgery were fixed with 10% neutral formalin for 24 h at room temperature and embedded in paraffin for 3 h at 60˚C. The clinicopathological characteristics of the patients are summarized in Table I, and the clinical stage of the patients was defined according to the criteria of the American Joint Committee on Cancer (AJCC 8th staging system). The present study was approved (approval no. KYLX2022075) by the Ethics Committee of the Third Affiliated Hospital of Kunming Medical University (Kunming, China) Written informed consent was provided by all patients participating in the present study.

Hematoxylin and eosin (H&E) staining. HE staining was used to evaluate histomorphology. After incubation at 60˚C for 3 h, paraffin-embedded tissue sections of 4~5 μm were dewaxed in xylene, and then the sections were placed successively in high to low concentrations of alcohol to hydrate the tissues. After staining the tissues with hematoxylin (cat. no. C0107; Beyotime Institute of Biotechnology) for 7 min at room temperature and eosin (cat. no. C0109; Beyotime Institute of Biotechnology) for 4 min at room temperature, the slices were dehydrated in an alcohol series from low to high concentrations, and then the tissues were cleared with xylene. After air drying, the slices were sealed with neutral gum, observed and photographed under a fluorescent microscope (cat. no. DMI4000B; Leica Microsystems GmbH).

Immunohistochemistry (IHC). IHC was used to analyze the expression of PPP1R14D protein in tissues. After baking at 60˚C for 3 h, the paraffin-embedded tissue sections were dewaxed in xylene and then hydrated with gradient alcohol. Tissue sections were placed in a solution of sodium citrate at pH 6.0, followed by high-pressure heat to repair the antigens. Endogenous peroxidase was removed by 3% H_2O_2. After sealing the non-specific binding site with 10% goat serum (cat. no. SP KIT-B3; MXB Biotechnologies, Inc.) for 30 min at room temperature, the primary PPP1R14D antibody (cat. no. HPA041846; Atlas Antibodies) was diluted with PBS at 1:200, and the tissue was incubated in the diluted antibody at 4˚C overnight. HRP-labeled secondary antibody working solution (Envision; cat. no. K5007; Dako; Agilent Technologies, Inc,). was incubated with the tissues at 37˚C for 30 min, and then 3,3-diaminobenzidine was used for color rendering (DAB; cat. no. K5007; Dako; Agilent Technologies, Inc,). Finally, the tissue was redyed with hematoxylin for 1 min, differentiated with 1% hydrochloric acid ethanol for 5 sec, blued with water for 30 min, dehydrated with gradient alcohol, dried transparently with xylene and sealed with neutral adhesive. Scans were performed using a fluorescent microscope (cat. no. DMI4000B). IHC scores were calculated based on

Table I. Clinicopathological characteristics of Spatients with lung adenocarcinoma were obtained (n=128).

Clinicopathological characteristic	Number (%)
Sex	
Male	66 (51.6)
Female	62 (48.4)
Age range, years	27-78
Mean age, years)	55
Age, years	
≤60	90 (70.3)
>60	38 (29.7)
Smoking history	
Yes	44 (34.4)
No	84 (65.6)
T stage[a]	
T1	60 (46.9)
T2	55 (43.0)
T3	10 (7.8)
T4	3 (2.3)
N classification[a]	
N0	100 (78.1)
N1	3 (2.35)
N2	22 (17.2)
N3	3 (2.35)
AJCC grading[a]	
I	81 (63.3)
II	20 (15.6)
III	27 (21.1)

[a]American Joint Committee on Cancer (AJCC 8th stage system).

the intensity and extent of staining observed under the microscope and determined independently by two pathologists who did not know the characteristics of patients. If there was a disagreement, the tissue was reviewed again until a consensus was reached. Scores of 0-3 were considered to indicate negative expression; scores of 4-6 indicated weak expression; and scores of 8-12 indicated strong expression. A score of >4-6 was considered positive.

Cell culture. The LUAD cell lines A549, PC-9, H1299 and H2342 and the human normal lung bronchial epithelial cell lines BEAS-2B and 16-HBE were purchased from the ATCC Cell Bank. A549 cells were cultured on DMEM F12 medium (cat. no. C11330500BT; Gibco; Thermo Fisher Scientific, Inc.) supplemented with 10% fetal bovine serum (cat. no. SA101.02; Cellmax; https://www.cellmaxcell.com). The other cell lines were cultured on RPMI-1640 medium (cat. no. C11875500BT; Gibco; Thermo Fisher Scientific, Inc.) supplemented with 10% fetal bovine serum. The working concentrations of penicillin and streptomycin (cat. no. P1400; Beijing Solarbio Science & Technology Co., Ltd.) added to the cell culture medium were 100 U/ml and 0.1 mg/ml, respectively. All cells were placed in an incubator containing 5% carbon dioxide and cultured at 37˚C.

Cell infection. The short hairpin (sh)PPP1R14D-1 (5'-TAG ATCCATGAGAGCTTCCAG-3'), shPPP1R14D-2 (5'-AAC TTGAGCATCCACCCATTG-3') and scramble control (5'-TTCTCCGAACGTGTCACGT-3') sequences were inserted into the GV248 lentiviral vector (cat. no. CON077; Shanghai GeneChem Co., Ltd.). The concentration of shPPP1R14D-1, shPPP1R14D-2 and Scramble was 4E + 8TU/ml, 4E + 8TU/ml and 5E + 8TU/ml, respectively. A549 and PC-9 cells were infected with the virus in 4% polybrene (cat. no. REVG005; Shanghai GeneChem Co., Ltd.) at a multiplicity of infection (MOI) of 20. After 72 h of infection, the cells were cultured in complete medium containing 2 μl/ml puromycin to screen stable cell lines for 48 h. The green fluorescent protein (GFP) tag was carried in the shRNA lentiviral vector and used to observe the infection efficiency of lentivirus under fluorescent microscope. When an infection efficiency >80% was observed, the cells were collected as experimental cells, and the lentivirus knockdown efficiency was detected by western blotting.

Western blot analysis. RIPA lysis buffer (cat. no. R0010; Beijing Solarbio Science & Technology Co., Ltd.) containing PMSF (cat. no. P0100; Beijing Solarbio Science & Technology Co., Ltd.) and protein phosphatase (cat. no. P1260; ApplyGen Technologies, Inc.) was used to lyse cells under ultrasound on ice. Total protein was collected after high-speed centrifugation (10,000 g) for 30 min at 4˚C, and the protein concentration was detected using a BCA kit (cat. no. 23227; Thermo Fisher Scientific, Inc.). Equal amounts of protein (30 ug) were separated on 12% SDS-PAGE gels and then transferred onto 0.22-μm PVDF membrane (cat. no. ISEQ00010; MilliporeSigma). The membrane was blocked with 5% skim milk (Skim milk powder was dissolved in TBST containing 1/1,000 Tween-20) for 2 h at room temperature to block non-specific sites, and it was incubated overnight with antibody dilution at 4˚C using the following antibodies: GAPDH (1:1,000; cat. no. 60004-1-IG; ProteinTech Group, Inc.), PPP1R14D (1:500; cat. no. HPA041846; Atlas Antibodies), c-Myc (1:1,000; cat. no. ab32072), CDK2 (1:1,000; cat. no. ab32147), Cyclin E1 (1:1,000; cat. no. ab33911), MMP2 (1:500; cat. no. ab92536), MMP9 (1:1,000; cat. no. ab76003), Vimentin (1:1,000; cat. no. ab92547), Kras (1:1,000; cat. no. ab275876), PKCα (1:1,000; cat. no. ab32376), BRAF (1:1,000; cat. no. ab33899), MEK1 (1:2,000; cat. no. ab32576), and phosphorylated (p)-MEK1 (1:1,000; cat. no. ab32088; all from Abcam), p-PKCα (1:1,000; cat. no. 9375T), p-BRAF (1:1,000; cat. no. 2696S), ERK1/2 (1:1,000; cat. no. 4695S) and p-ERK (1:2,000; cat. no. 4370S; all from Cell Signalling Technology, Inc.). The membrane was washed with TBST three times for 10 min each time and then incubated with a specific secondary antibody at room temperature for 1 h, mainly containing anti-mouse IgG (1:10,000; cat. no. SA00001-1) and anti-rabbit IgG (1:10,000; cat. no. Sa00001-2; both from ProteinTech Group, Inc.). After washing three times for 15 min each time, the protein positive bands were visualized using ECL (cat. no. WB KLS0100; MilliporeSigma) and finally quantitated using ImageJ software (version 1.51K; National Institutes of Health). The experiment was carried out three times, with GAPDH as an internal reference.

3-(4,5-Dimethylthiazol-2-yl)-5-(3-carboxymethoxyphenyl)-2-(4-sulfophenyl)-2H- tetrazolium (MTS) assay. Scramble-, shPPP1R14D-1- and shPPP1R14D-2-infected cells were inoculated into 96-well plates with a 100-μl culture system of 1,500 cells/well and then cultured in an incubator. Then, 20 μl/well MTS (cat. no. G111A; Promega Corporation) reaction working solution (MTS: PMS=20:1) was added on the 1st, 2nd, 3rd, 4th, 5th and 6th days and incubated for 2 h at 37˚C. The OD value of the cells was determined at 490 nm. A total of five wells were used for each treatment group per experiment, and the experiment was repeated three times.

Colony formation assay. Scramble-, shPPP1R14D-1- and shPPP1R14D-2-infected cells were inoculated into six-well plates with a 2-ml culture system of 300 cells/well and then cultured in an incubator for 10-14 days. The minimum number of cells forming a colony was 50. When the clones were visible to the naked eye, the cells were fixed with methanol for 30 min at room temperature, stained with Giemsa (cat. no. G1015; Beijing Solarbio Science & Technology Co., Ltd.) for 30 min at room temperature and washed thoroughly with water. Colonies were counted using ImageJ software (version 1.51K; National Institutes of Health). The experiment was repeated three times.

5-ethynyl-2'-deoxyuridine (EdU) staining assay. Scramble-, shPPP1R14D-1- and shPPP1R14D-2-infected cells were inoculated into 24-well plates with a 1-ml culture system and then cultured in an incubator. When the cell density reached 70~80%, the cells were incubated with medium containing 50 μM EdU for 2 h. The cells were immobilized with 4% formaldehyde for 30 min and permeated with 0.5% Triton X-100 for 10 min, followed by staining for EdU and all nuclei (cat. no. C10310-1; Guangzhou RiboBio Co., Ltd.). A fluorescence microscope (cat. no. DMI4000B) was used to observe and capture images of the cells. EdU-positive cells were counted using ImageJ software (National Institutes of Health). The experiment was repeated three times.

Cell cycle analysis by flow cytometry. Scramble-, SHPPP1R14D-1- and SHPPP1R14D-2-infected cells were treated with serum starvation synchronization, serum-containing medium was added to culture cells for 12 h, and cells were collected into a 5-ml flow tube and washed twice with precooled PBS when the cell density reached 80%. After 70% alcohol was fixed at 4˚C for 24 h, the cells were washed twice with precooled PBS. Cells were stained according to the instructions of the cell cycle kit (cat. no. C1052; Beyotime Institute of Biotechnology). The cell cycle distribution was detected using a flow cytometer (BD FACS Aria™11; BD Biosciences) and BD-FACS Diva 6.0 software and the results were analyzed using ModFit LT 3.2 software. The experiment was repeated three times.

Wound-healing assays. Scramble-, shPPP1R14D-1- and shPPP1R14D-2-infected cells were inoculated into a six-well plate, under which they were marked with a horizontal line in advance. When the cells were full of six-well plates, a long wound was marked perpendicular to the horizontal line with a 10-μl spear head. PBS was used to wash the floating cells, and 2-ml serum-free medium was added to continue the cell culture. The wound area was observed and images were captured under a microscope at 0, 24 and 48 h. The areas of the wound were calculated using ImageJ software (National Institutes of Health). The experiment was repeated three times.

Transwell migration assays. Scramble-, shPPP1R14D-1- and shPPP1R14D-2-infected cells were seeded in 200-μl serum-free medium of $2.5x10^4$ cells (A549) or $1x10^5$ cells (PC-9) in the upper chamber, and 600 μl medium supplemented with 10% FBS was added to the lower chamber. The cells were incubated within 24 h. Then, the cells were fixed with methanol for 30 min at room temperature and stained with Giemsa for 30 min at room temperature. Cells passing through the membrane were counted using ImageJ software (National Institutes of Health). The experiment was repeated three times.

Matrigel invasion assays. Scramble-, shPPP1R14D-1- and shPPP1R14D-2-infected cells were seeded in 150-μl serum-free medium of $2.5x10^4$ cells (A549) or $1.5x10^5$ cells (PC-9) in the upper chamber, and 600 μl medium supplemented with 10% FBS (A549) or 20% FBS (PC-9) was added to the lower chamber. Matrigel (cat. no. 356234; BD Biosciences) was diluted with serum-free medium at 1:8, and then 65 μl diluent was added to cover the upper chamber and dried at 37˚C for 4-5 h. The cells were incubated within 24 h. Then, the cells were fixed with methanol for 30 min at room temperature and stained with Giemsa for 30 min at room temperature. Cells passing through the membrane were counted using ImageJ software (National Institutes of Health). The experiment was repeated three times.

Nude mouse xenograft assay. The animal experiment was conducted according to the guidelines set by the Animal Experimental Ethical Committee of Kunming Medical University, and the animal experiment was approved by the Animal Experimental Ethical Committee of Kunming Medical University (approval no. KMMU2021749). The nude mouse xenograft model was used to evaluate cell growth *in vivo*. Female SPF grade BALB/c nude mice (n=10) weighing between 18 and 22 g, aged 4-5 weeks-old, were obtained and bred in the Animal Experimental Center of Kunming Medical University. All mice were reared in an animal room at a temperature of 25˚C and 50% humidity under a 12/12 h light/dark cycle. All mice were allowed free access to food and water. Nude mice were randomly divided into the scramble group and the shPPP1R14D-1 group (five mice per group). Each nude mouse was subcutaneously injected with $1x10^7$ infected cells/100 μl in the right axilla. The length and width of the tumor were measured with Vernier calipers every week, and the tumor volume was calculated by the formula length x width ^{2}/2.

Human endpoints were reached when the xenograft tumor reached >10% of the animal body weight, the tumor diameter was >20 mm, tumors metastasized or grew such that it led to rapid body weight loss (>20%), or signs of immobility, a huddled posture, inability to eat, ruffled fur, self-mutilation, ulceration, infection or necrosis were observed. The mice that reached study endpoints were sacrificed by CO_2 euthanasia with 50% displacement of cage volume/min. Sacrifice was confirmed

by observation of unconsciousness, absence of heartbeat and absence of breathing for 20 min. All experimental mice were euthanized by CO_2 after 6 weeks (June 2021), and tumors were dissected and separated.

Statistical analysis. All experiments were repeated three times. Count data are expressed as percentages, and measurement data are expressed as the mean ± standard deviation ($\overline{X}$ ± SD). The log-rank test was used to analyze the survival outcome of patients in Kaplan-Meier plotter database. Pearson's chi-square test was used to analyze the IHC results. Unpaired Student's t-test was used to compare the means of two groups of data. One-way ANOVA was used to compare multiple groups, the LSD (equal Variances) and Tamhane's T2 (unequal Variances) test were used for the post-hoc pairwise comparisons after the Homogeneity of variance test. All statistics were analyzed using SPSS 23.0 software (IBM Corp.). P<0.05 was considered to indicate a statistically significant difference. Data were visualized with GraphPad Prism 6.0 software (GraphPad Software, Inc.).

Results

PPP1R14D is overexpressed in LUAD and associated with poor prognosis. Using GEPIA database analysis, it was found that PPP1R14D was highly expressed in LUAD tissue, while PPP1R14D was expressed at low levels in LUSC tissue (Fig. 1A). For further study, 128 cases of LUAD tissues and their adjacent normal lung tissues were collected. After H&E staining was performed to determine the tissue type (Fig. 1B), IHC was used to detect the difference in PPP1R14D expression between LUAD tissues and normal lung tissues and it was identified that the protein expression level of PPP1R14D in LUAD was higher than that in adjacent lung tissues (Fig. 1C). Correlations between PPP1R14D protein expression and LUAD clinicopathologic features were further analyzed. It was revealed that the expression of PPP1R14D was negatively correlated with the age of the patients. More importantly, the expression of PPP1R14D was positively correlated with the AJCC stage of the patients (P<0.05; Table II), while there was no correlation between PPP1R14D expression and sex, smoking history, tumor T stage or N stage (P>0.05). In addition, the Kaplan-Meier Plotter database was used for survival analysis and it was identified that the OS and PFS of LUAD patients with high PPP1R14D expression were significantly shorter than those with low PPP1R14D expression (Fig. 1D). However, PPP1R14D expression had no significant effect on OS and PFS in LUSC patients (Fig. S1). The aforementioned data indicated that PPP1R14D overexpression may be relevant to the tumorigenesis and progression of LUAD.

Knockdown of PPP1R14D expression inhibits LUAD cell proliferation in vitro. To explore the underlying roles of the PPP1R14D gene in promoting the development of LUAD, the basic expression level of PPP1R14D protein was first measured in LUAD cell lines, including A549, PC-9, H1299, and H2342 and the normal bronchial epithelial cell lines BEAS-2B and 16-HBE. The results showed that PPP1R14D was highly expressed in LUAD cells but expressed at low levels in normal bronchial epithelial cell lines (Fig. 2A). The A549 and PC-9 cell lines were selected for further experiments. PPP1R14D-knockdown cells with corresponding controls were constructed, since they are not only highly expressed PPP1R14D, but also susceptible to lentiviral infection. Compared with the Scramble group, lentivirus shPPP1R14D-1 and shPPP1R14D-2 successfully infected cells (Fig. S2) and significantly knocked down the endogenous expression of PPP1R14D in A549 and PC-9 cells (Fig. 2B). The MTS assay results indicated that knockdown of PPP1R14D significantly suppressed the growth of A549 and PC-9 cells (Fig. 2C). The EdU assay results revealed that the ratio of EdU-positive cells was significantly decreased in A549 and PC-9 cells after PPP1R14D knockdown (Fig. 2D and E). The colony formation assay results showed that the colony formation abilities of PPP1R14D knockdown cells were significantly decreased (Fig. 2F and G). These results suggested that PPP1R14D promotes the proliferation of LUAD cells.

Knockdown of PPP1R14D expression induces LUAD cell cycle arrest at the G1 phase. To analyze the effect of PPP1R14D on the cell cycle, a flow cytometric assay was conducted after knockdown of PPP1R14D expression. It was found that the percentage of cells in G1 phase of the A549 cell cycle increased from 61.21 (Scramble) to 76.20 or 77.13% (shPPP1R14D), and the percentage of cells in G1 phase of the PC-9 cell cycle increased from 84.74% (Scramble) to 92.55 or 95.57% (shPPP1R14D) (Fig. 3A-C). It was found that knockdown of PPP1R14D in A549 and PC-9 cells significantly reduced the expression of the G1 phase-related proteins c-Myc, CDK2 and Cyclin E1 (Fig. 3D-F). These results indicated that PPP1R14D promotes the proliferation of LUAD cells by regulating the G1 phase of the cell cycle.

Knockdown of PPP1R14D expression inhibits LUAD cell migration and invasion in vitro. To evaluate the effect of PPP1R14D on migration and invasion, a series of experiments were conducted. Wound-healing assays showed that knockdown of PPP1R14D expression inhibited wound closure compared with the Scramble (Fig. 4A). Transwell migration and invasion assays also showed that knockdown of PPP1R14D expression resulted in lower cell migration and invasion rates, respectively, compared with the Scramble (Fig. 4B, C, E and F). It was found that knockdown of PPP1R14D expression in A549 and PC-9 cells significantly reduced the expression of the migration- and invasion-related proteins MMP2, MMP9 and Vimentin (Fig. 4D). These results indicated that PPP1R14D promotes the migration and invasion of LUAD cells by regulating the expression of migration- and invasion-related proteins.

Knockdown of PPP1R14D inhibits tumorigenicity and growth of LUAD cells in vivo. To evaluate the effect of PPP1R14D on the tumorigenesis and proliferation of LUAD cells *in vivo*, a nude mouse xenograft assay was performed. The results showed that the tumor formation speed of A549 cells after PPP1R14D knockdown was significantly slower than that of the Scramble group from the fourth week (P<0.05; Fig. 5A and B), and the final volume and weight of tumors in the shPPP1R14D-1 group were also significantly smaller and lower than those in the Scramble group (P<0.05; Fig. 5C and D). IHC staining

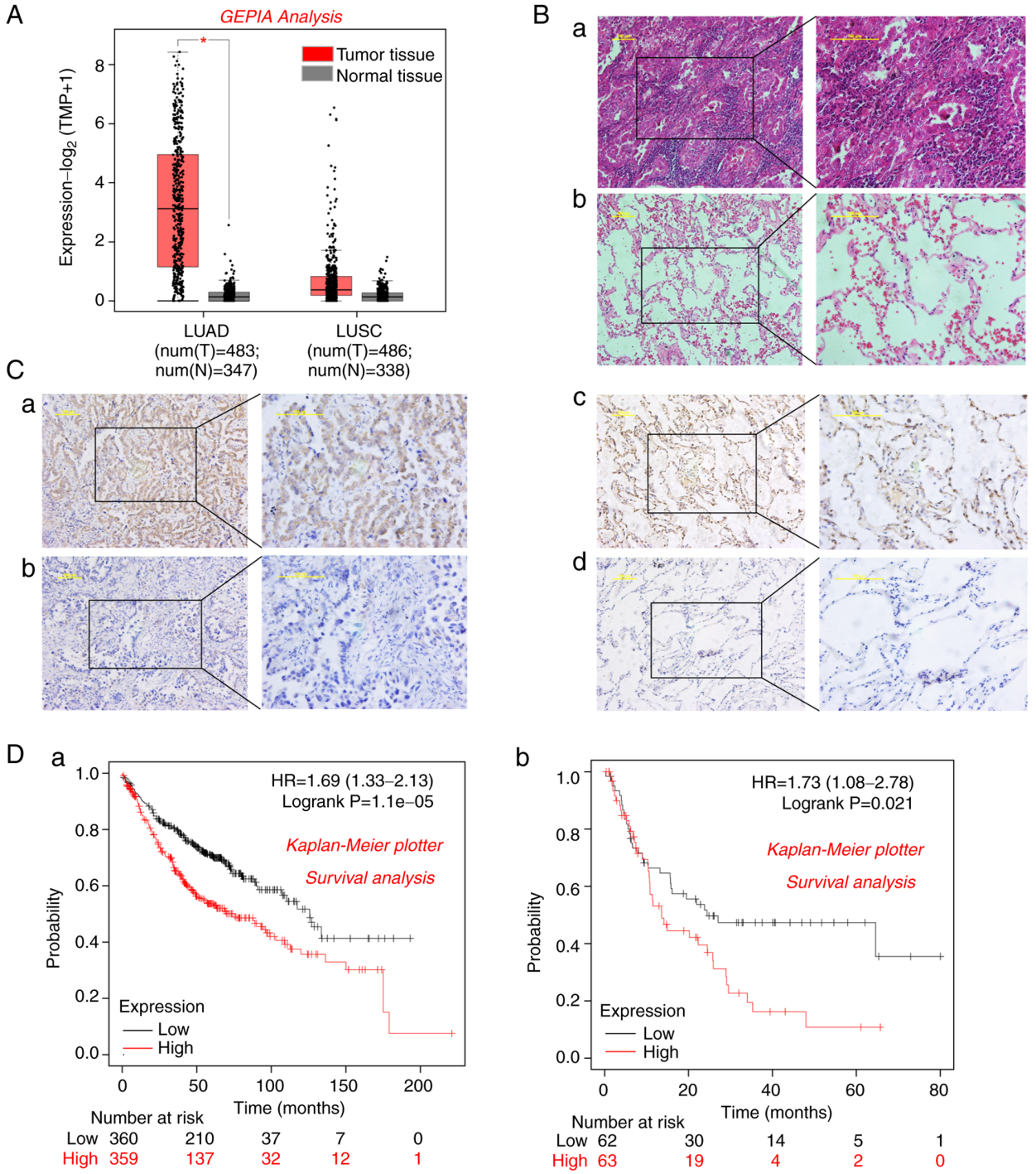

Figure 1. PPP1R14D is overexpressed in LUAD and is associated with poor prognosis. (A) GEPIA dataset analysis revealed that the expression of PPP1R14D in LUAD was significantly higher than that in normal lung tissue. Student's t-test, *P<0.05. (B) H&E staining to verify (a) LUAD tissue and paired (b) normal lung tissue (scale bar, 100 μm). (C) PPP1R14D expression in LUAD and normal lung tissue, as detected by immunohistochemical staining (scale bar, 100 μm); a, Positive PPP1R14D staining in LUAD tissue; b, Negative PPP1R14D staining in LUAD tissue; c, Positive PPP1R14D staining in normal lung tissue and d, Negative PPP1R14D staining in normal lung tissue. (D) Kaplan-Meier plotter database predicted the survival rates of LUAD patients with high and low PPP1R14D expression; a, overall survival; b, progression-free survival. PPP1R14D, protein phosphatase 1 regulatory subunit 14D; LUAD, lung adenocarcinoma; HR, hazard ratio.

showed that PPP1R14D protein expression was weakened in xenograft tumors with PPP1R14D knockdown compared with the Scramble group (Fig. 5E). These results indicated that PPP1R14D promotes the occurrence and development of LUAD by increasing the proliferation of LUAD cells *in vivo* and that inhibiting PPP1R14D can reduce the growth of LUAD.

Knockdown of PPP1R14D suppresses the PKCα/BRAF/MEK/ERK signaling pathway. To elucidate the underlying mechanism by which PPP1R14D knockdown inhibits proliferation, migration and invasion in LUAD, the levels of key proteins were evaluated by western blotting. The results showed that PPP1R14D knockdown significantly reduced the expression levels of BRAF, p-BRAF, p-MEK1 and p-ERK1/2

Table II. Associations between the clinical characteristics and PPP1R14D expression in LUAD.

Clinicopathological characteristic	Number	Expression of PPP1R14D		P-value
		Positive, N (%)	Negative, N (%)	
Primary tumors of LUAD	128	77 (60.2)	51 (39.8)	0.001
Paired normal lung tissues	128	40 (31.2)	88 (68.8)	
Sex				0.538
Male	66	38 (57.6)	28 (42.4)	
Female	62	39 (62.9)	23 (37.1)	
Age, years				0.021
≤60	90	60 (66.7)	30 (33.3)	
>60	38	17 (47.7)	21 (55.3)	
Smoking history				0.859
Yes	44	26 (59.1)	18 (40.9)	
No	84	51 (60.7)	33 (39.3)	
T stage				0.914
T1+ T2	115	69 (60.0)	46 (40.0)	
T3 + T4	13	8 (61.5)	5 (38.5)	
N stage				0.070
N0	100	56 (56.0)	44 (44.0)	
N1 + N2 + N3	28	21 (75.0)	7 (25.0)	
AJCC stage				0.035
I + II	101	56 (55.4)	45 (44.6)	
III	27	21 (77.8)	6 (22.2)	

PPP1R14D, protein phosphatase 1 regulatory subunit 14D; LUAD, lung adenocarcinoma; AJCC, American Joint Committee on Cancer.

proteins. The expression of Ras, a common upstream activating protein in the RAF-MEK-ERK pathway, was not significantly changed with PPP1R14D knockdown. However, p-PKCα, another protein regulating the RAF-MEK-ERK signaling pathway, was significantly downregulated ($P<0.05$; Fig. 6). These results indicated that PPP1R14D could specifically activate the PKCα/BRAF/MEK/ERK signaling pathway to affect the proliferation, migration and invasion of LUAD cells.

Discussion

PPP1R14D is a member of the inhibitory subfamily of protein phosphatase 1 regulatory subunits (16,20). Several studies have confirmed that dysregulation of PP1 regulatory subunits with PP1 inhibitory function, including the PPP1R14 family, is closely related to tumor development. Jin *et al* (21) found that active PPP1R14A could inhibit the expression of the tumor suppressor protein Merlin and drive the activity of Ras to promote carcinogenic transformation of tumors. Zhao *et al* (22) have shown that high expression of PPP1R14B can promote the proliferation and metastasis of gliomas and their drug resistance to temozolomide. PPP1R14C is considered to be a promoter of triple-negative breast and prostate cancers (23,24). Previously, it has been suggested that PPP1R14D may play a carcinogenic role in pancreatic cancer and breast cancer (18,19). However, the function of PPP1R14D in LUAD has not been investigated individually.

The present study confirmed that PPP1R14D was not differentially expressed in LUSC tissues and normal lung tissues and that it had no effect on the OS and PFS of LUSC patients, but PPP1R14D was overexpressed in LUAD and that high expression of PPP1R14D was associated with higher AJCC stage and shorter OS and PFS. This implies that PPP1R14D overexpression is closely associated with poor prognosis in LUAD patients. To clarify the biological functions of PPP1R14D in LUAD, it was first confirmed that PPP1R14D expression was also increased in LUAD cells compared with the normal lung bronchial epithelial cells. Then, A549 and PC-9 cells with high PPP1R14D expression were selected for knockdown of PPP1R14D expression via infection with PPP1R14D shRNA lentivirus.

It is well known that the most basic feature of cancer is the uncontrolled proliferation of cancer cells caused by abnormal activity in the cell cycle (25). In addition, for tumors to metastasize and grow, they must invade and migrate to surrounding tissues (26). The present results showed that PPP1R14D knockdown inhibited the proliferation of LUAD cells *in vitro* and *in vivo*. Moreover, PPP1R14D knockdown arrested the A549 and PC-9 cell cycle in G1 phase and reduced the expression of the G1-related proteins c-Myc, CDK2 and Cyclin E1. It was also confirmed that knockdown of PPP1R14D inhibited

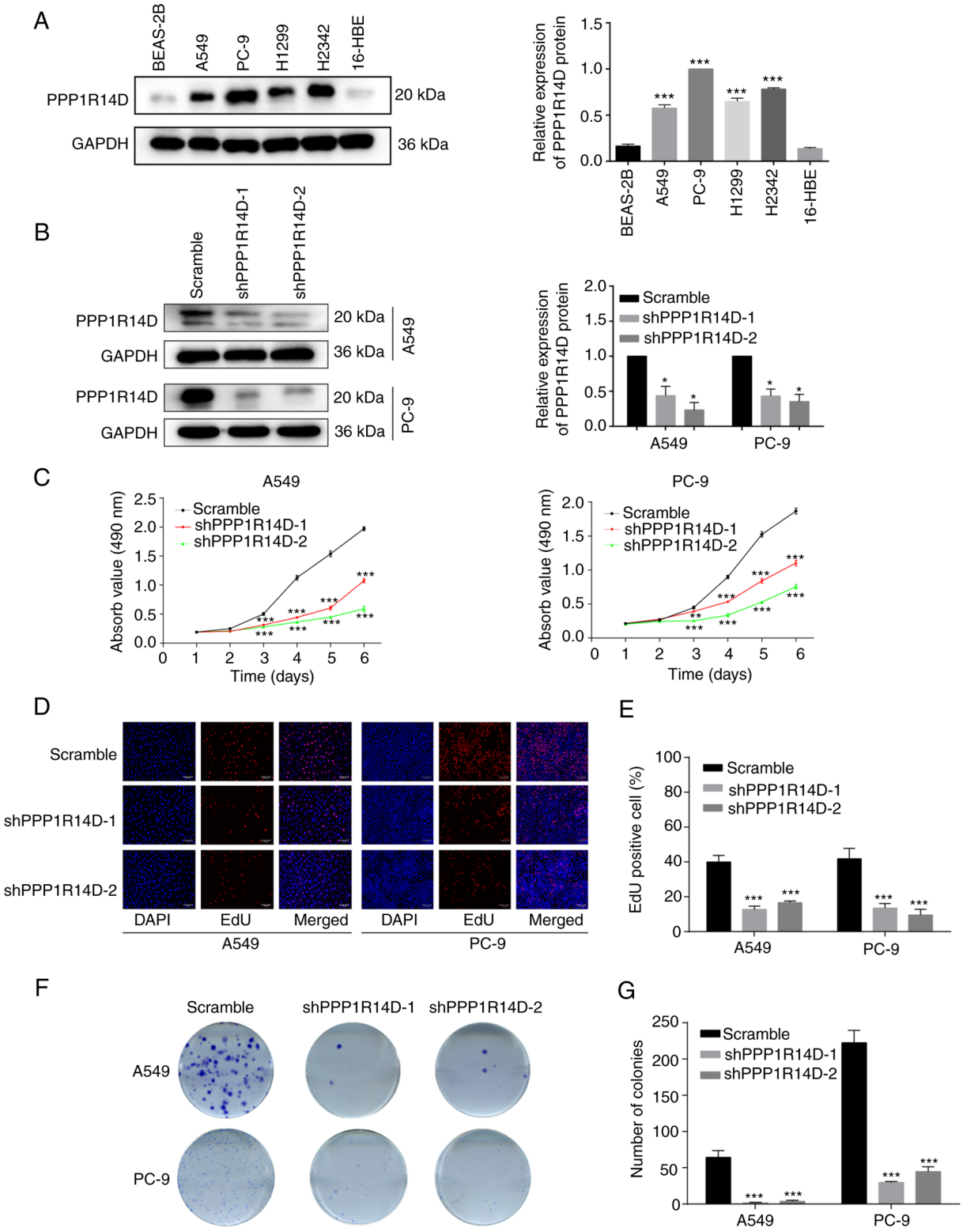

Figure 2. Knockdown of PPP1R14D inhibits the proliferation of LUAD cells. (A) Levels of PPP1R14D protein in LUAD and normal bronchial epithelial cell lines. GAPDH was used as the loading control. One-way ANOVA, ***P<0.001 vs. BEAS-2B or 16-HBE cells. (B) Western blot analysis of PPP1R14D protein expression in A549 and PC-9 cells infected with PPP1R14D shRNA lentivirus. GAPDH was used as the loading control. One-way ANOVA, *P<0.05 vs. Scramble. (C-G) PPP1R14D knockdown significantly inhibited the proliferation of A549 and PC-9 cells, as evaluated by (C) MTS assay, (D and E) EdU assay (scale bar, 100 μm) and (F and G) colony formation assays. One-way ANOVA; **P<0.01 and ***P<0.001 vs. Scramble. PPP1R14D, protein phosphatase 1 regulatory subunit 14D; LUAD, lung adenocarcinoma; sh-short hairpin.

the migration and invasion of A549 and PC-9 cells *in vitro* and reduced the expression of the migration- and invasion-related proteins MMP2, MMP9 and Vimentin. However, due to experimental limitations, the effect of PPP1R14D on migration and invasion *in vivo* was not verified, which is a limitation to the present study.

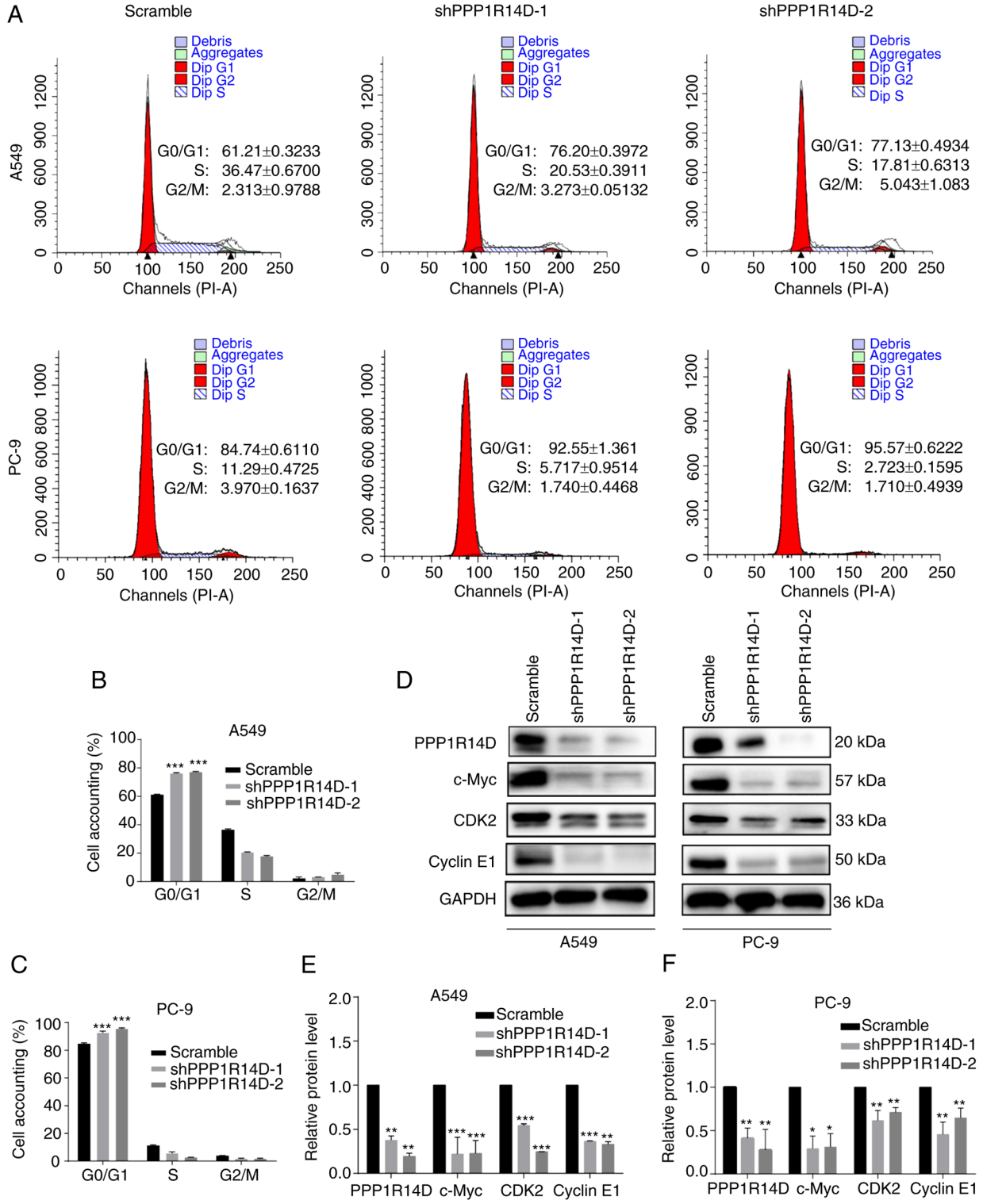

Figure 3. Knockdown of PPP1R14D induces LUAD cell arrest at the G1 phase. (A-C) Flow cytometric analysis of A549 and PC-9 cells. (D-F) The G1 phase-related proteins c-Myc, CDK2 and Cyclin E1 were significantly downregulated after knockdown of PPP1R14D in A549 and PC-9 cells. GAPDH was used as the loading control. One-way ANOVA; *P<0.05, **P<0.01 and ***P<0.001 vs. Scramble. PPP1R14D, protein phosphatase 1 regulatory subunit 14D; LUAD, lung adenocarcinoma; sh-short hairpin.

c-Myc, a protooncogene, is dysregulated or abnormally activated in almost 50% of human cancers and regulates cancer cell growth by targeting CDK2 and Cyclin E, which are essential for the transition from G1 to S phase of the cell cycle (27-30). Members of the MMP2 and MMP9 matrix metalloproteinase superfamily degrade the extracellular matrix primarily through its proteolytic function and promote tumor growth, angiogenesis, migration and invasion, and metastasis to distant organs (31-34). Vimentin is an important intermediate filament protein that is commonly expressed in mesenchymal cells and is one of the essential components of the cytoskeleton (35). Increasing evidence suggests that the

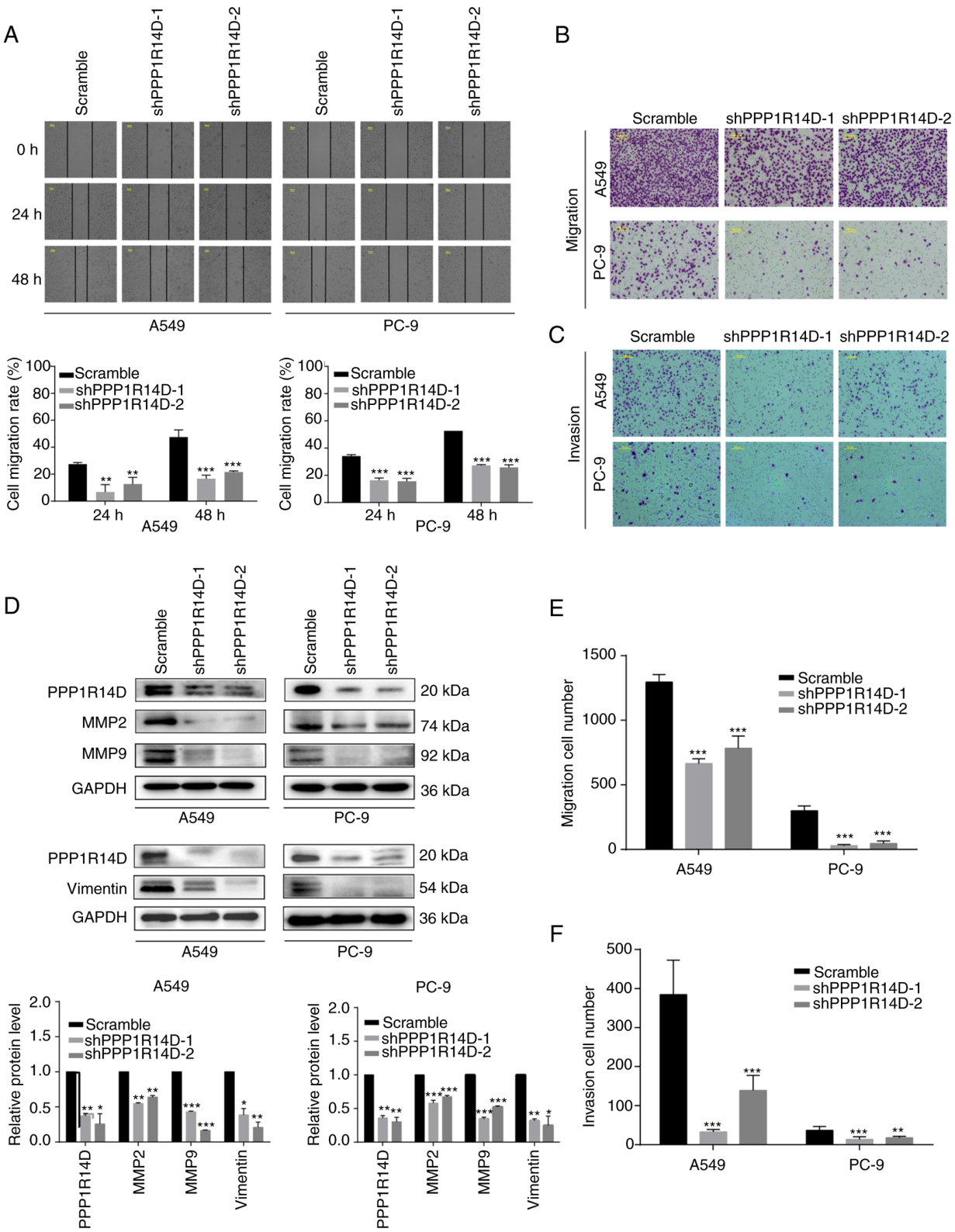

Figure 4. Knockdown of PPP1R14D inhibits the migration and invasion of LUAD cells. (A) Wound-healing assays were performed to evaluate the migration of cells, and the percentage of wound closure was calculated (scale bar, 100 μm). (B and E) Transwell and (C and F) Matrigel assays showed the effect of PPP1R14D expression levels on the migration and invasion abilities, respectively, of LUAD cells (scale bar, 100 μm). (D) The migration- and invasion-related proteins MMP2, MMP9 and Vimentin were significantly downregulated after knockdown of PPP1R14D in A549 and PC-9 cells. GAPDH was used as the loading control. One-way ANOVA; *P<0.05, **P<0.01, ***P<0.001 vs. Scramble. PPP1R14D, protein phosphatase 1 regulatory subunit 14D; LUAD, lung adenocarcinoma; sh-short hairpin.

abnormal expression of Vimentin in epithelial cancer cells may be related to local invasiveness and metastatic potential, and multiple steps of the metastatic cascade are directly or indirectly regulated by Vimentin (36). There is clear evidence

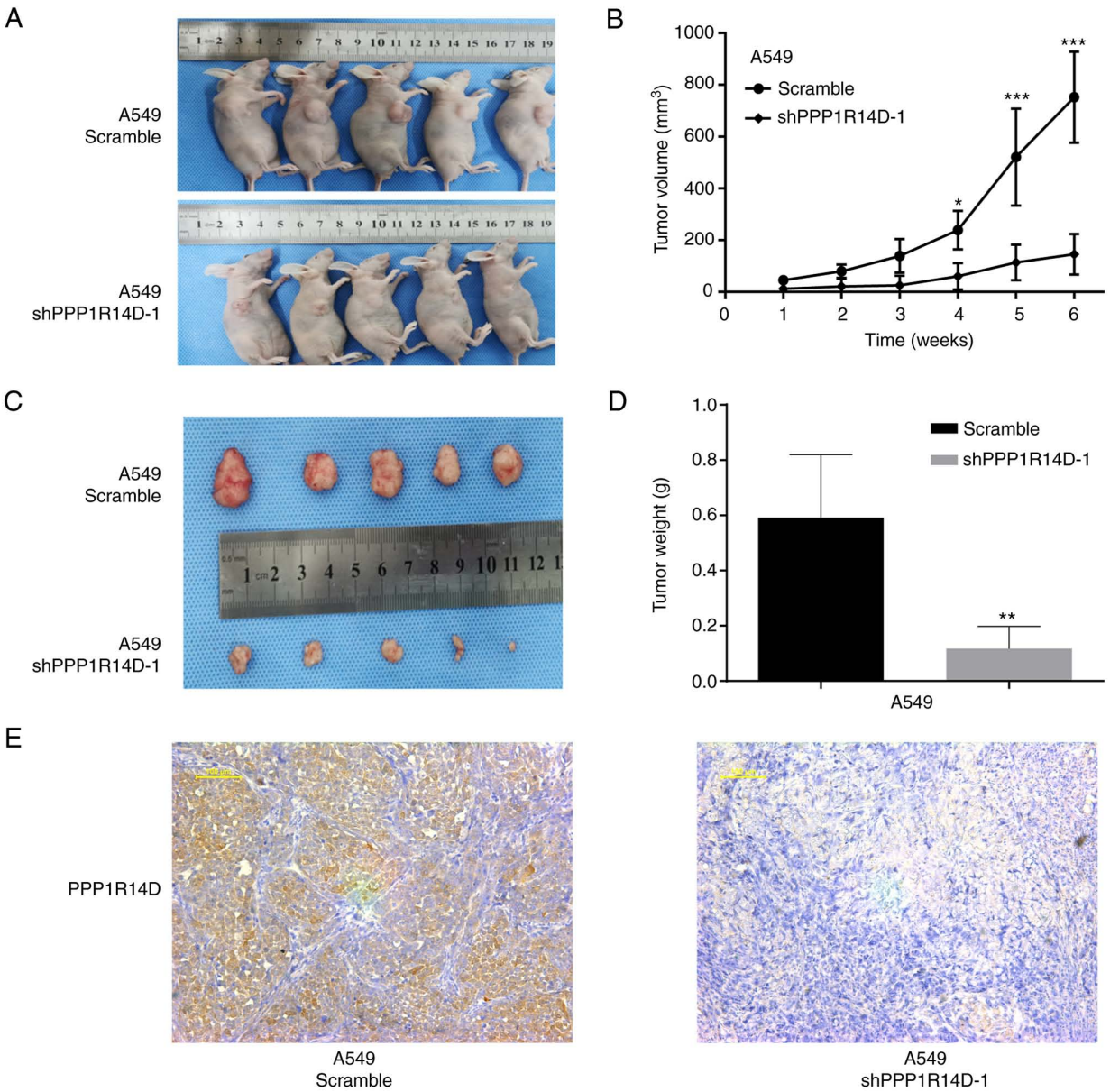

Figure 5. Knockdown of PPP1R14D inhibits tumorigenesis and growth of A549 cells *in vivo*. (A) General view of subcutaneous tumorigenesis in nude mice. (B) Growth curve, (C) volume and (D) weight of tumor xenografts. (E) Representative immunohistochemical staining of PPP1R14D protein expression in xenograft tumors (scale bar, 100 μm). Student's t-test; *P<0.05, **P<0.01 and ***P<0.001 vs. Scramble. PPP1R14D, protein phosphatase 1 regulatory subunit 14D; sh-short hairpin.

that Vimentin expression is associated with increased metastasis, reduced survival and poor prognosis in patients with NSCLC (37).

The ERK/MAPK pathway regulates a variety of cellular activities, including cell growth and signal transduction (38). A large number of studies have shown that the ERK/MAPK pathway in cancer can regulate the expression of c-Myc mRNA and promote the stability of c-Myc, thus promoting the growth of cancer cells (39-42). In addition, the ERK/MAPK signaling can increase tumor invasion and metastasis by upregulating the expression of MMP2 and MMP9 (43-45). Therefore, expression levels of proteins related to the ERK/MAPK signaling pathway were detected, and the results revealed that after PPP1R14D knockdown, BRAF, p-BRAF, p-MEK1 and p-ERK1/2 protein levels decreased. However, PPP1R14D knockdown did not significantly change the expression of Ras, a common upstream activating protein in the RAF-MEK-ERK pathway. Therefore, it can be observed that PPP1R14D knockdown did reduce the expression of BRAF/MEK/ERK signaling pathway proteins. Since several previous studies (39-45) have shown that the ERK/MAPK signaling pathway acts as upstream proteins to regulate c-MYc, MMP2 and MMP9 proteins, it was hypothesized that the reduced expression of c-Myc, MMP2 and MMP9 proteins was regulated by ERK/MAPK signaling pathway after PPP1R14D knockdown. However, the internal mechanism of the ERK/MAPK signaling pathway in regulating c-Myc, MMP2 and MMP9 proteins after PPP1R14D knockdown was not thoroughly explored, which is a further limitation to the current study.

As the central hub of numerous signal transduction processes, protein kinase C (PKC) is involved in the regulation of gene expression, proliferation, survival, apoptosis, migration

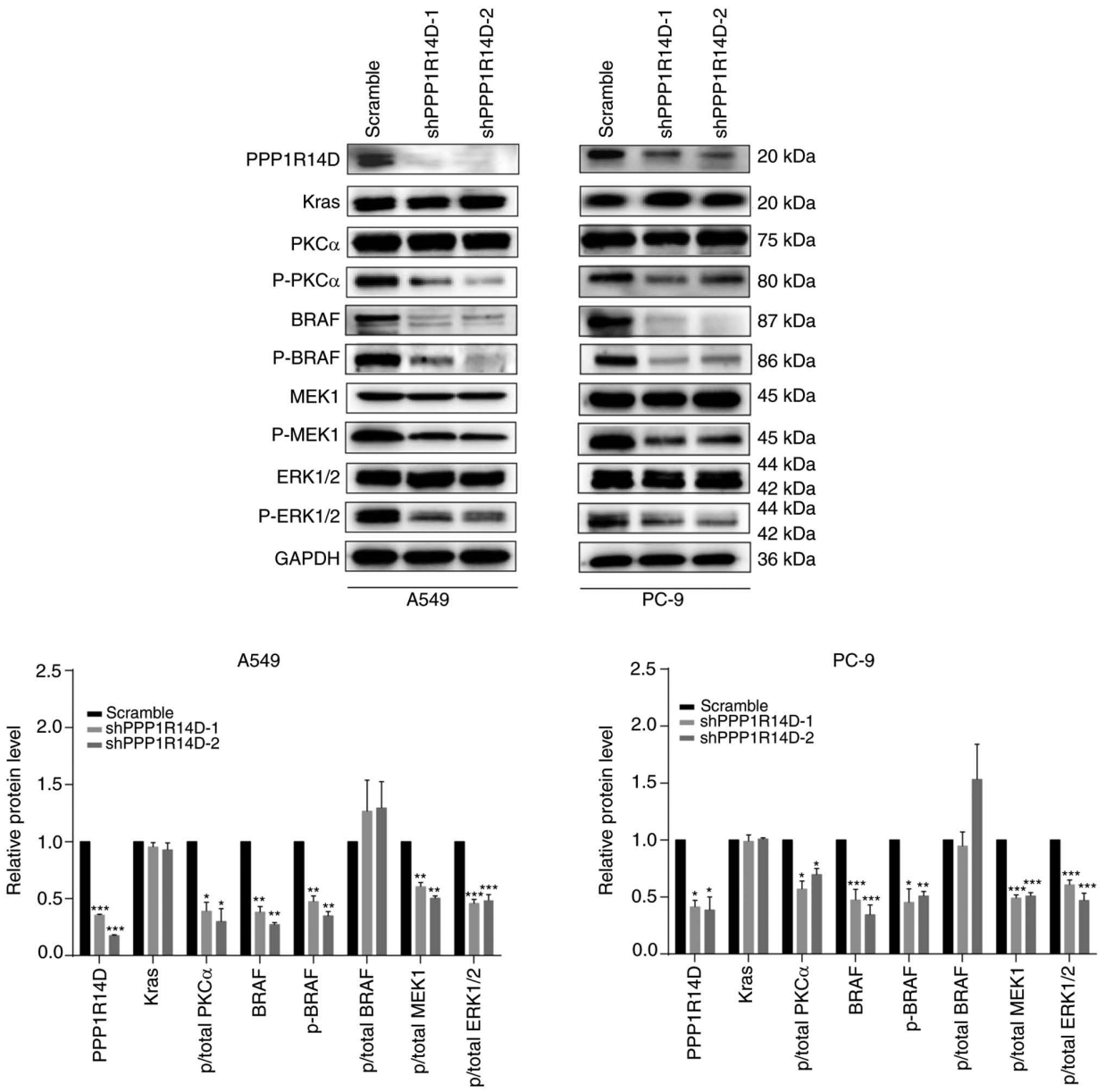

Figure 6. Knockdown of PPP1R14D suppresses the PKCα/BRAF/MEK/ERK signaling pathway. Downregulation of PPP1R14D reduced the levels of p-PKCα, BRAF, p-BRAF, p-MEK1, and p-ERK1/2. GAPDH was used as a loading control. One-way ANOVA; *P<0.05, **P<0.01 and ***P<0.001 vs. Scramble. PPP1R14D, protein phosphatase 1 regulatory subunit 14D; p-, phosphorylated.

and other cellular processes (46). In fact, in addition to being activated by Ras proteins, the ERK/MAPK signaling pathway can also be activated by PKCα in cancer (13,14). Therefore, PKCα was detected at the protein level and it was found that p-PKCα decreased significantly after PPP1R14D knockdown.

PPP1R14D is a PP1 inhibitor dependent on PKC regulation. PKC binds to PPP1R14D and subsequently phosphorylates PPP1R14D at Thr58 to inhibit PP1 activity. Notably, the results of the present study showed that PPP1R14D reversed PKC regulation; that is, PPP1R14D knockdown decreased p-PKCα. It was hypothesized that PPP1R14D reversed the regulation of PKCα by affecting PP1. Previous studies have provided a plausible explanation for our hypothesis. It has been reported that active PP1 can lead to a decrease in PKCα activity (47). Importantly, Luo *et al* previously found that protein phosphatase 1 regulatory subunit 1A (PPP1R1A) can lead to an increase in PKCα phosphorylation levels by inhibiting PP1 activity, while knocking down PPP1R1A leads to a decrease in p-PKCα (48). Therefore, the downregulation of p-PKCα caused by PPP1R14D knockdown is probably caused by the increase in PP1 activity.

In summary, PPP1R14D expression is significantly increased in LUAD and associated with poor prognosis in patients. PPP1R14D may promote the proliferation, migration and invasion of LUAD by activating the PKCα/BRAF/MEK/ERK signaling pathway. It was hypothesized that the activation of the PKCα/BRAF/MEK/ERK signaling pathway may be related to PPP1R14D's inhibition of PP1. However, the limitation to the present study is that the direct evidence that PPP1R14D regulates the biological function of LUAD by inhibiting PP1 is not sufficient and requires further exploration in the future. Further studies

on how PPP1R14D affects PP1 will be clarified in future studies, including detection of PP1 expression and activity, construction of mutants and certain rescue experiments. Finally, it is worth emphasizing that the present results suggested that PPP1R14D may be involved in the occurrence and development of LUAD and could be a potential therapeutic target in LUAD.

Acknowledgements

The authors express their gratitude to all members of the Department of Cancer Biotherapy Center Laboratory of the Third Affiliated Hospital of Kunming Medical University.

Funding

The present study was partially supported by the National Natural Science Foundation of China (grant nos. 81660389 and 81602029), the Scientific Research Fund of Education Department of Yunnan Province (grant no. 2022J0212) and the Joint Special Funds for the Department of Science and Technology of Yunnan Province-Kunming Medical University (grant no. 202201AY070001-144).

Availability of data and materials

The datasets used and/or analyzed during the current study are available from the corresponding author upon reasonable request.

Authors' contributions

HC, CG, HY, and YW designed the experiments. ZW and LY collected the specimens, performed IHC and analyzed the clinical data. HC, ZW, RL and TD performed the other experiments. TL, YX and JG provided technical support in this research project. KL and RL analyzed the statistical data. TD, ZF and YL assembled and installed the figures. CG and HY supervised the study and confirm the authenticity of all the raw data. HC wrote the manuscript. All authors read and approved the final version of the manuscript.

Ethics approval and consent to participate

Ethical approval (approval no. KYLX2022075) for the use of human paraffin-embedded tissue was granted by the Ethics Committee of the Third Affiliated Hospital of Kunming Medical University (Kunming, China). Written informed consent was provided by all patients participating in the present study. The animal experiment was approved (approval no. KMMU2021749) by the Animal Experimental Ethical Committee of Kunming Medical University.

Patient consent for publication

Not applicable.

Competing interests

The authors declare that they have no competing interests.

References

1. Sung H, Ferlay J, Siegel RL, Laversanne M, Soerjomataram I, Jemal A and Bray F: Global cancer statistics 2020: GLOBOCAN estimates of incidence and mortality worldwide for 36 cancers in 185 countries. CA Cancer J Clin 71: 209-249, 2021.
2. Kleczko EK, Kwak JW, Schenk EL and Nemenoff RA: Targeting the complement pathway as a therapeutic strategy in lung cancer. Front Immunol 10: 954, 2019.
3. Lu T, Yang X, Huang Y, Zhao M, Li M, Ma K, Yin J, Zhan C and Wang Q: Trends in the incidence, treatment, and survival of patients with lung cancer in the last four decades. Cancer Manag Res 11: 943-953, 2019.
4. Hirsch FR, Scagliotti GV, Mulshine JL, Kwon R, Curran WJ Jr, Wu YL and Paz-Ares L: Lung cancer: Current therapies and new targeted treatments. Lancet 389: 299-311, 2017.
5. Duffy MJ and Crown J: Biomarkers for predicting response to immunotherapy with immune checkpoint inhibitors in cancer patients. Clin Chem 65: 1228-1238, 2019.
6. Zheng Q, Min S and Zhou Q: Identification of potential diagnostic and prognostic biomarkers for LUAD based on TCGA and GEO databases. Biosci Rep 41: BSR20204370, 2021.
7. Denisenko TV, Budkevich IN and Zhivotovsky B: Cell death-based treatment of lung adenocarcinoma. Cell Death Dis 9: 117, 2018.
8. Liu WJ, Du Y, Wen R, Yang M and Xu J: Drug resistance to targeted therapeutic strategies in non-small cell lung cancer. Pharmacol Ther 206: 107438, 2020.
9. Zhang J, Sun B, Ruan X, Hou X, Zhi J, Meng X, Zheng X and Gao M: Oncoprotein HBXIP promotes tumorigenesis through MAPK/ERK pathway activation in non-small cell lung cancer. Cancer Biol Med 18: 105-119, 2021.
10. Dasgupta P, Kulkarni P, Bhat NS, Majid S, Shiina M, Shahryari V, Yamamura S, Tanaka Y, Gupta RK, Dahiya R and Hashimoto Y: Activation of the Erk/MAPK signaling pathway is a driver for cadmium induced prostate cancer. Toxicol Appl Pharmacol 401: 115102, 2020.
11. Zhang G, Luo X, Wang Z, Xu J, Zhang W, Chen E, Meng Q, Wang D, Huang X, Zhou W and Song Z: TIMP-2 regulates 5-Fu resistance via the ERK/MAPK signaling pathway in colorectal cancer. Aging (Albany NY) 14: 297-315, 2022.
12. Samatar AA and Poulikakos PI: Targeting RAS-ERK signalling in cancer: Promises and challenges. Nat Rev Drug Discov 13: 928-942, 2014.
13. Mahapatra L, Andruska N, Mao C, Gruber SB, Johnson TM, Fullen DR, Raskin L and Shapiro DJ: Protein kinase C-α is upregulated by IMP1 in melanoma and is linked to poor survival. Melanoma Res 29: 539-543, 2019.
14. Lin R, Bao X, Wang H, Zhu S, Liu Z, Chen Q, Ai K and Shi B: TRPM2 promotes pancreatic cancer by PKC/MAPK pathway. Cell Death Dis 12: 585, 2021.
15. Awad MM, Liu S, Rybkin, II, Arbour KC, Dilly J, Zhu VW, Johnson ML, Heist RS, Patil T, Riely GJ, *et al*: Acquired resistance to $KRAS^{G12C}$ inhibition in cancer. N Engl J Med 384: 2382-2393, 2021.
16. Liu QR, Zhang PW, Lin Z, Li QF, Woods AS, Troncoso J and Uhl GR: GBPI, a novel gastrointestinal- and brain-specific PP1-inhibitory protein, is activated by PKC and inactivated by PKA. Biochem J 377: 171-181, 2004.
17. Aggen JB, Nairn AC and Chamberlin R: Regulation of protein phosphatase-1. Chem Biol 7: R13-R23, 2000.
18. Zhang W, Shang S, Yang Y, Lu P, Wang T, Cui X and Tang X: Identification of DNA methylation-driven genes by integrative analysis of DNA methylation and transcriptome data in pancreatic adenocarcinoma. Exp Ther Med 19: 2963-2972, 2020.
19. Dang M, Armbruster N, Miller MA, Cermeno E, Hartmann M, Bell GW, Root DE, Lauffenburger DA, Lodish HF and Herrlich A: Regulated ADAM17-dependent EGF family ligand release by substrate-selecting signaling pathways. Proc Natl Acad Sci USA 110: 9776-9781, 2013.
20. Eto M: Regulation of cellular protein phosphatase-1 (PP1) by phosphorylation of the CPI-17 family, C-kinase-activated PP1 inhibitors. J Biol Chem 284: 35273-35277, 2009.
21. Jin H, Sperka T, Herrlich P and Morrison H: Tumorigenic transformation by CPI-17 through inhibition of a merlin phosphatase. Nature 442: 576-579, 2006.
22. Zhao M, Shao Y, Xu J, Zhang B, Li C and Gong J: LINC00466 impacts cell proliferation, metastasis and sensitivity to temozolomide of glioma by sponging miR-137 to regulate PPP1R14B expression. Onco Targets Ther 14: 1147-1159, 2021.

23. Jian Y, Kong L, Xu H, Shi Y, Huang X, Zhong W, Huang S, Li Y, Shi D, Xiao Y *et al*: Protein phosphatase 1 regulatory inhibitor subunit 14C promotes triple-negative breast cancer progression via sustaining inactive glycogen synthase kinase 3 beta. Clin Transl Med 12: e725, 2022.
24. Grey J, Jones D, Wilson L, Nakjang S, Clayton J, Temperley R, Clark E, Gaughan L and Robson C: Differential regulation of the androgen receptor by protein phosphatase regulatory subunits. Oncotarget 9: 3922-3935, 2017.
25. Dang F, Nie L and Wei W: Ubiquitin signaling in cell cycle control and tumorigenesis. Cell Death Differ 28: 427-438, 2021.
26. Yang S, Zhang JJ and Huang XY: Orai1 and STIM1 are critical for breast tumor cell migration and metastasis. Cancer Cell 15: 124-134, 2009.
27. Salvi N (ed): Intrinsically disordered proteins: Dynamics, binding, and function. Elsevier, 2019.
28. Xu C and Zheng J: siRNA against TSG101 reduces proliferation and induces G0/G1 arrest in renal cell carcinoma-involvement of c-myc, cyclin E1, and CDK2. Cell Mol Biol Lett 24: 7, 2019.
29. Santoni-Rugiu E, Falck J, Mailand N, Bartek J and Lukas J: Involvement of Myc activity in a G(1)/S-promoting mechanism parallel to the pRb/E2F pathway. Mol Cell Biol 20: 3497-3509, 2000.
30. Berns K, Hijmans EM and Bernards R: Repression of c-Myc responsive genes in cycling cells causes G1 arrest through reduction of cyclin E/CDK2 kinase activity. Oncogene 15: 1347-1356, 1997.
31. Geng X, Chen C, Huang Y and Hou J: The prognostic value and potential mechanism of matrix metalloproteinases among prostate cancer. Int J Med Sci 17: 1550-1560, 2020.
32. Andersson P, Yang Y, Hosaka K, Zhang Y, Fischer C, Braun H, Liu S, Yu G, Liu S, Beyaert R, *et al*: Molecular mechanisms of IL-33-mediated stromal interactions in cancer metastasis. JCI Insight 3: e122375, 2018.
33. Jiang H and Li H: Prognostic values of tumoral MMP2 and MMP9 overexpression in breast cancer: A systematic review and meta-analysis. BMC Cancer 21: 149, 2021.
34. Buttacavoli M, Di Cara G, Roz E, Pucci-Minafra I, Feo S and Cancemi P: Integrated multi-omics investigations of metalloproteinases in colon cancer: Focus on MMP2 and MMP9. Int J Mol Sci 22: 12389, 2021.
35. Schaedel L, Lorenz C, Schepers AV, Klumpp S and Köster S: Vimentin intermediate filaments stabilize dynamic microtubules by direct interactions. Nat Commun 12: 3799, 2021.
36. Kidd ME, Shumaker DK and Ridge KM: The role of vimentin intermediate filaments in the progression of lung cancer. Am J Respir Cell Mol Biol 50: 1-6, 2014.
37. Havel LS, Kline ER, Salgueiro AM and Marcus AI: Vimentin regulates lung cancer cell adhesion through a VAV2-Rac1 pathway to control focal adhesion kinase activity. Oncogene 34: 1979-1990, 2015.
38. Morrison DK and Davis RJ: Regulation of MAP kinase signaling modules by scaffold proteins in mammals. Annu Rev Cell Dev Biol 19: 91-118, 2003.
39. Meyer N and Penn LZ: Reflecting on 25 years with MYC. Nat Rev Cancer 8: 976-990, 2008.
40. Albihn A, Johnsen JI and Henriksson MA: MYC in oncogenesis and as a target for cancer therapies. Adv Cancer Res 107: 163-224, 2010.
41. Chu J, Li Y, Deng Z, Zhang Z, Xie Q, Zhang H, Zhong W and Pan B: IGHG1 regulates prostate cancer growth via the MEK/ERK/c-Myc pathway. Biomed Res Int 2019: 7201562, 2019.
42. Wang Y, Yang S, Zhang S and Wu X: Oxymatrine inhibits proliferation and migration of vulvar squamous cell carcinoma cells via attenuation of the RAS/RAF/MEK/ERK pathway. Cancer Manag Res 12: 2057-2067, 2020.
43. Lin F, Chengyao X, Qingchang L, Qianze D, Enhua W and Yan W: CRKL promotes lung cancer cell invasion through ERK-MMP9 pathway. Mol Carcinog 54 (Suppl 1): E35-E44, 2015.
44. Qin H, Liu X, Li F, Miao L, Li T, Xu B, An X, Muth A, Thompson PR and Zhang X: PAD1 promotes epithelial-mesenchymal transition and metastasis in triple-negative breast cancer cells by regulating MEK1-ERK1/2-MMP2 signaling. Cancer lett 409: 30-41, 2017.
45. Zhang H, Shen B, Swinarska JT, Li W, Xiao K and He P: 9-Hydroxypheophorbide α-mediated photodynamic therapy induces matrix metalloproteinase-2 (MMP-2) and MMP-9 down-regulation in Hep-2 cells via ROS-mediated suppression of the ERK pathway. Photodiagnosis Photodyn Ther 11: 55-62, 2014.
46. Isakov N: Protein kinase C (PKC) isoforms in cancer, tumor promotion and tumor suppression. Semin Cancer Biol 48: 36-52, 2018.
47. Ricciarelli R and Azzi A: Regulation of recombinant PKC alpha activity by protein phosphatase 1 and protein phosphatase 2A. Arch Biochem Biophys 355: 197-200, 1998.
48. Luo W, Xu C, Ayello J, Dela Cruz F, Rosenblum JM, Lessnick SL and Cairo MS: Protein phosphatase 1 regulatory subunit 1A in ewing sarcoma tumorigenesis and metastasis. Oncogene 37: 798-809, 2018.